Journal of Biomedical Optics

SPIEDigitalLibrary.org/jbo

Evaluating the use of optical coherence tomography for the detection of epithelial cancers *in vitro*

Louise E. Smith
Vanessa Hearnden
Zenghai Lu
Rod Smallwood
Keith D. Hunter
Stephen J. Matcher
Martin H. Thornhill
Craig Murdoch
Sheila MacNeil

SPIE

Evaluating the use of optical coherence tomography for the detection of epithelial cancers *in vitro*

Louise E. Smith,[a,b] Vanessa Hearnden,[a,c] Zenghai Lu,[a] Rod Smallwood,[d] Keith D. Hunter,[e] Stephen J. Matcher,[a] Martin H. Thornhill,[c] Craig Murdoch,[c] and Sheila MacNeil[a]
[a]University of Sheffield, Kroto Research Institute, Department of Engineering Materials, North Campus, Broad Lane, Sheffield, S3 7HQ, United Kingdom
[b]University of South Australia, Mawson Institute, Mawson Lakes Campus, Mawson Lakes Boulevard, Mawson Lakes, 5095, Australia
[c]University of Sheffield, School of Clinical Dentistry, Academic Unit of Oral and Maxillofacial Medicine and Surgery, Sheffield, S10 2TA, United Kingdom
[d]University of Sheffield, Department of Computer Science, Regent Court, 211 Portobello, Sheffield S1 4DP, United Kingdom
[e]University of Sheffield, School of Clinical Dentistry, Academic Unit of Oral and Maxillofacial Pathology, Sheffield, S10 2TA, United Kingdom

Abstract. Optical coherence tomography (OCT) is a noninvasive imaging methodology that is able to image tissue to depths of over 1 mm. Many epithelial conditions, such as melanoma and oral cancers, require an invasive biopsy for diagnosis. A noninvasive, real-time, point of care method of imaging depth-resolved epithelial structure could greatly improve early diagnosis and long-term monitoring in patients. Here, we have used tissue-engineered (TE) models of normal skin and oral mucosa to generate models of melanoma and oral cancer. We have used these to determine the ability of OCT to image epithelial differences *in vitro*. We report that while *in vivo* OCT gives reasonable depth information for both skin and oral mucosa, *in vitro* the information provided is less detailed but still useful. OCT can provide reassurance on the development of TE models of skin and oral mucosa as they develop *in vitro*. OCT was able to detect the gross alteration in the epithelium of skin and mucosal models generated with malignant cell lines but was less able to detect alteration in the epithelium of TE models that mimicked oral dysplasia or, in models where tumor cells had penetrated into the dermis. [DOI: 10.1117/1.3652708]

Keywords: optical coherence tomography; melanoma; oral cancer; noninvasive imaging; tissue engineering; skin; oral dysplasia.

Paper 11161R received Apr. 1, 2011; revised manuscript received Sep. 2, 2011; accepted for publication Sep. 22, 2011; published online Oct. 27, 2011.

1 Introduction

Optical coherence tomography (OCT) is a noninvasive method of imaging that utilizes the high penetration of long wavelength light. OCT, often referred to as optical ultrasound, measures backscattered and reflected light from different tissue structures within a tissue sample. Differences in the optical properties and reflectivity of tissue components create distinguishable signals from different depths of the sample. OCT is currently and widely used in ophthalmology as the optical properties of the eye make it relatively easy to image compared to other tissues, which have higher light scattering properties. It is hoped that the technical advances that have allowed OCT to be increasingly used in ophthalmology may extend to other areas of diagnostics and imaging.

There is an increasing need for the development of methodologies for noninvasive imaging of tissues both for *in vitro* tissue engineering purposes and clinically for disease diagnostics, monitoring of tissue repair, and tissue reconstruction. We have previously reported using swept-source OCT (SS-OCT) to monitor re-epithelialization and wound healing in our reconstructed skin constructs.[1,2]

Address all correspondence to: Sheila MacNeil, University of Sheffield, Kroto Research Institute, North Campus - Broad Lane, Sheffield, South Yorkshire S3 7HQ, United Kingdom; Tel: +44(0)114 2225995; Fax: +44(0)114 222 5945; E-mail: s.macneil@shef.ac.uk.

OCT is increasingly being used to monitor the development of oral cancer, oral mucositis, and basal cell carcinoma in the papillary dermis *in* vivo.[3–7] It is also being used to monitor the development of tissue-engineered (TE) models or oral mucosa and to noninvasively monitor skin. For example, Boppart et al.[8–10] used an Nd:YVO_4-pumped Ti-Saph laser with a resolution of 10 μm to monitor the *in vitro* migration of murine macrophages through a matrigel matrix; while others have used OCT to monitor the development of TE skin composed of epidermal keratinocytes on top of a fibroblast-populated amorphous collagen gel.[11,12]

Previous work from our laboratory has shown that OCT can effectively monitor the development of an epithelium in a TE skin model based on human dermis[1] and can also be used to monitor wound healing in this model.[2] We suggest that the three-dimensional (3D) models we have developed[13] provide excellent test-beds in which to explore the limits of discrimination of OCT for tumor cells.

The aim of this study was to assess the ability of OCT to detect epithelial disruption due to the presence of metastatic melanoma and early invasive oral cancer in 3D tissue-engineered constructs *in vitro*. To this end, we compared OCT and histological images from skin and mucosal models generated with carcinoma and dysplastic cell lines to those generated with normal oral or skin

1083-3668/2011/16(11)/116015/8/$25.00 © 2011 SPIE

keratinocytes, and as a reference, we compared these images to those of skin and oral mucosa from a normal healthy volunteer.

2 Materials and Methods

2.1 *Primary Cell Culture*

Skin keratinocytes and human skin dermal fibroblasts were harvested from split thickness skin grafts (STSGs) obtained from specimens following routine breast reductions and abdominoplasties (Ethical Committee of the Northern General Hospital Trust, Sheffield, United Kingdom, Ref: 06/Q2306/25). Oral keratinocytes and oral fibroblasts were extracted from buccal tissue obtained from consenting patients during routine dental surgeries [Sheffield Research Ethics Committee approval (Ref: 07/H1309/105)]. Cell extraction was performed as previously described in Refs. 13 and 14.

Skin and oral keratinocytes were grown in Green's medium consisting of Dulbecco's modified eagles medium (DMEM) and Ham's F12 medium in a 3:1 ratio supplemented with 10% (v/v) foetal calf serum (FCS), 100 IU/ml penicillin, 100 μg/ml streptomycin, 0.625 μg/ml amphotericin B, 6.25 μg/ml adenine, 10 ng/ml epidermal growth factor, 1.36 ng/ml triidothyronine, 5 μg/ml transferrin, 5 μg/ml insulin, 0.4 μg/ml hydrocortisone, and 8.5 ng/ml cholera toxin. Dermal and oral fibroblasts were grown in fibroblast culture medium (FCM) consisting of DMEM supplemented with 10% (v/v) foetal calf serum (FCS), 100 IU/ml penicillin, 100 μg/ml streptomycin, and 0.625 μg/ml amphotericin B. All reagents were purchased from Sigma-Aldrich, United Kingdom, except FCS, which was purchased from Biowest Biosera, United Kingdom. All cells were cultured at 37°C in a 5% CO_2/95% air humidified incubator. Passage 1 to 3 keratinocytes and passage 4 to 9 fibroblasts were used in all experiments.

2.2 *Human Melanoma Cell Culture*

Three human metastatic melanoma cell lines were used, HBL, A375-SM, and C8161. The HBL cell line was derived from a lymph node metastasis of a nodular melanoma. Cells were maintained in Ham's F10 medium supplemented with 5% (v/v) FCS, 5% (v/v) newborn calf serum, 2 mM L-glutamine, 100 IU/ml penicillin, plus 100 μg/ml streptomycin. The A375-SM cell line was a kind gift from Professor M. J. Humphries (University of Manchester, United Kingdom). The A375 cell line was established in culture from a lymph node metastasis of a 54-year-old female. The C8161 cell line was derived from an abdominal wall metastasis from a post-menopausal woman with recurrent malignant melanoma and was donated by M. Edwards (University of Glasgow, United Kingdom). Both A375-SM and C8161 cells were cultured in Eagle's modified essential media supplemented with 10% (v/v) FCS, 2 mM L-glutamine, 100 IU/ml penicillin, 100 μg/ml streptomycin, 1.2 μg/ml amphotericin B, 1.5% (v/v) (100 × stock) vitamin concentrate, 1 mM sodium pyruvate, and 10% (v/v) nonessential amino acids.

2.3 *Oral Cancer Cell Lines*

The D20 dysplastic cell line was kindly donated by Dr. Keith Hunter (University of Sheffield, United Kingdom).[15,16] D20 cells were cultured in Green's medium (as previously described for keratinocytes). The SCC9 cell line was originally isolated from the tongue of a patient with squamous cell carcinoma (SCC) and cultured in a 1:1 ratio of DMEM: Ham's F12, supplemented with 10% FCS, 0.4 μg/ml hydrocortisone, 100 IU/ml penicillin, 100 μg/ml streptomycin, and 0.625 μg/ml amphotericin B. Cal27 is a squamous cell carcinoma human cell line isolated from the tongue of a patient with squamous cell carcinoma (ATCC, Manassas, Virginia).

2.4 *Production of TE Models*

STSGs were obtained during routine plastic surgery breast reduction and abdominoplasty operations or obtained from the Euro-Skin Bank (Netherlands). Glycerol was removed from Euro-Skin by extensive washing in phosphate buffered saline (PBS) and then both the STSG and Euro-Skin were immersed in sterile 1 M sodium chloride for 18 h at 37°C, resulting in an acellular de-epidermized human dermis (DED). The DED was thoroughly washed with PBS and placed into FCM. The DED was cut into squares approximately 2 × 2 cm and the papillary surface was orientated uppermost in Corning Costar 3516 6-well plates (Corning Inc., United Kingdom). Tissue-engineered skin and oral mucosa models were produced using a modified version of the method of Chakrabarty et al.[17] In brief, 1×10^5 dermal or 5×10^5 oral fibroblasts and 1×10^6 epithelial or 5×10^5 oral keratinocytes were seeded in Green's media into a medical stainless steel ring placed onto the papillary surface of the DED. After 48 h in submerged culture, the constructs were raised to an air-liquid interface and cultured in Green's medium for up to 22 days. For models containing melanoma cells in addition to the 1×10^6 keratinocytes, 5×10^5 melanoma cells were also added to the models. For models of oral carcinoma, 2.5×10^5 oral cancer cells were added to the model instead of 5×10^5 oral keratinocytes.

Media changes were performed every three to four days, or more frequently if the media was visibly depleted, indicated by a color change from red-purple to orange-yellow. For routine histology, constructs were transferred to 10% phosphate-buffered formaldehyde at room temperature. Samples were processed, embedded in paraffin wax, sectioned to a thickness of 4 μm, mounted, and stained using haematoxylin and eosin (H&E).

2.5 *OCT Imaging of TE Models*

Imaging of all of the TE models was performed using a SS-OCT system that is based on a Michelson Diagnostics Ltd. swept-source OCT data acquisition system (Michelson Diagnostics, Kent, United Kingdom) coupled to a Thorlabs LSM03 scan lens and in-house fiber interferometer (Thorlabs, Cambridgeshire, United Kingdom) with the models maintained in their standard six-well tissue culture plastic dishes. Imaging was performed through the tissue culture plastic lid to keep the TE models sterile and viable. The SS-OCT system was a Fourier domain OCT device, meaning that the images could be taken faster than with traditional time domain OCT. The light source was a Santec HSL-2000-10 wide sweep-laser with a wavelength of 1305 nm ± 15 nm with a sweep range of 150 nm. The OCT system uses an imaging engine (light source, detectors, PC/DAQ and software) adapted from a Michelson Diagnostics Ltd. EX1301 system. The interferometer and sample arm optics are built in-house using an SMF-28 beam splitter and circulator and a Thorlabs OCT

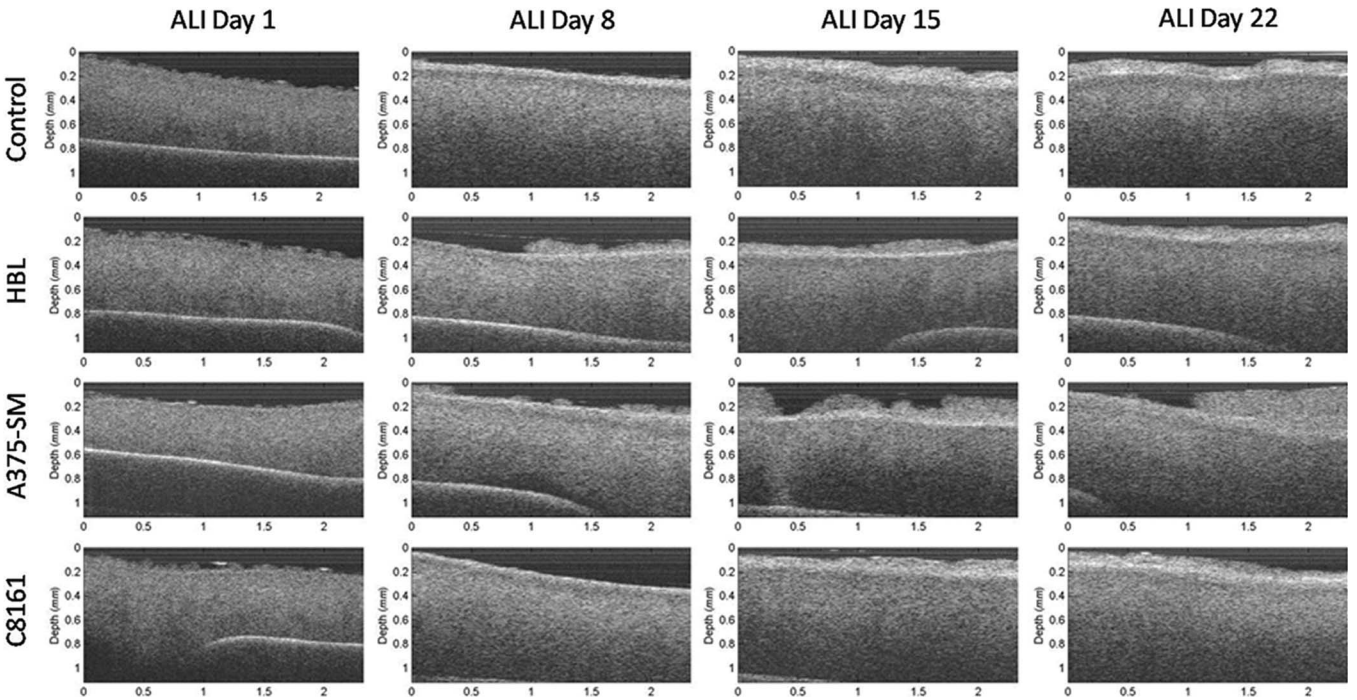

Fig. 1 Representative SS-OCT images of reconstructed skin developing over 22 days. HBL melanoma, A375-SM, and C8161 melanoma cells were also added to the reconstructed skin. Changes to the epidermis can be seen from day 8 onward when the HBL and A375-SM cells are in the reconstructed skin. There do not appear to be any differences when the C8161 cells are added.

objective and galvo scanners. The lateral resolution, in the plane of best focus, of the OCT system is defined by the Thorlabs LSM03 objective in the sample arm. In air, we measured a modulation depth of 45% using Element 1 of Group 5 in the USAF 1951 test target. For a Gaussian beam, this implies a full width half maximum (FWHM) spot size of around 15 μm. With the culture dish lid inserted, the modulation fell to 30%, implying a degradation of the FWHM spot size to 18 μm. This is most likely due to spherical and higher-order beam aberrations. The axial point spread function FWHM in air was measured to be 6.4 μm, degrading to 7.5 μm with the lid inserted. Mostly, this was due to uncompensated optical dispersion as it could be restored to 6.7 μm by inserting a matching lid into the reference arm (however, this was not done for these experiments). The overall dynamic range of this system was measured at 94 dB using a 10-kHz A-scan rate. The tissue culture plastic lids were left in place to ensure sterility of these experiments and also gently heated to remove any condensation before imaging and as required during imaging. Three TE models of each type were imaged in multiple sites toward the middle of the models. Only representative images are shown.

3 Results

3.1 *Ability of OCT to Detect Changes in Reconstructed Skin Due to the Presence of Melanoma*

Figure 1 shows representative SS-OCT images of the TE skin as it develops over 22 days after being raised to an air-liquid interface. The upper panel shows the controlled TE skin throughout 22 days of culture. The three lower panels show experiments in which melanoma cells were added, imaging the constructs at days 1, 8, 15, and 22. HBL cells are minimally invasive cells and as seen in Fig. 1 appear to cause minor changes to the structure of the epidermis. The A375-SM cells are moderately invasive and appear to cause a marked amount of disruption to the epidermis. The C8161 cells are highly invasive but in Fig. 1 do not appear to affect the reconstructed skin.

Figure 2 compares the images obtained from reconstructed skin with and without melanoma after 22 days of culture to the accompanying H&E histology. In the controlled reconstructed skin, the SS-OCT [Fig. 2(a)] and histology images [Fig. 2(b)] both show a progressively differentiated epidermis that is attached to the underlying dermis. This also appears to be the case when the HBL cells are added to the reconstructed skin model. When A375-SM cells are added to the reconstructed skin model, there are significant changes to the SS-OCT image [Fig. 2(e)] and these are mirrored in the histology [Fig. 2(f)]. There is an additional darker, less scattered layer above the epidermis. The histology suggests that these are lightly attached melanoma cells that have not entered the epidermis. Moving on to C8161 cells, these are highly metastatic and invade into the papillary dermis [as can be seen in the inset to Fig. 2(g)] that cannot be seen in the OCT image [Fig. 2(g)].[18,19] This invasion of melanoma cells into the dermis does not cause any visible disruption of the epidermal layer.

3.2 *Ability of OCT to Detect Changes in Reconstructed Oral Epithelia Due to the Presence of Oral Squamous Cell Carcinoma Cell Lines*

Figure 3 shows the appearance of three oral squamous cell carcinoma (OSCC) models and our TE oral mucosa when imaged

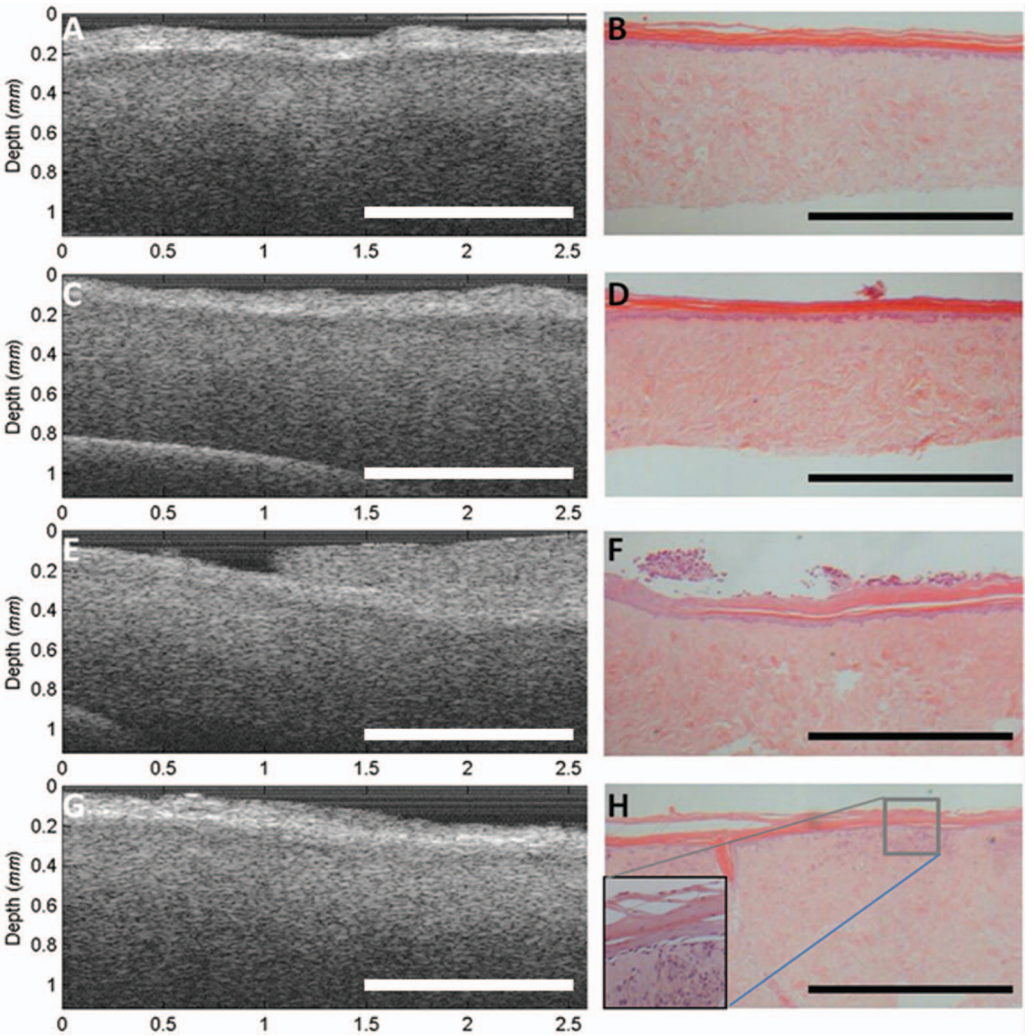

Fig. 2 (a) Representative SS-OCT image of reconstructed skin and (b) accompanying histology. (c) Representative SS-OCT image of reconstructed skin + HBL melanoma cells and (d) accompanying histology. (e) Representative SS-OCT image of reconstructed skin + A375-SM melanoma cells and (f) accompanying histology. (g) Representative SS-OCT image of reconstructed skin + C8161 melanoma cells and (h) accompanying histology. All images were taken after the models had been at an air-liquid interface for 22 days. All histology stained with H&E. Scale bar = 1 mm.

using OCT and traditional histological methods. Figure 3(a) shows a complete epithelium that is confirmed in the accompanying histology [Fig. 3(b)]. In all four OCT images, the epithelium can be distinguished from the connective tissue component as there is a difference in brightness due to an increase in backscattered light (with the connective tissue appearing brighter). This gives information about the thickness of the epithelium, which is often altered in pre-cancerous lesions (dysplasia). More subtle features and individual cells within the epithelia could not be distinguished using OCT. In Fig. 3(c), variations in the levels of brightness can be seen in the epithelium. This could potentially be explained by the accompanying histology [Fig. 3(d)], where islands of terminally differentiated cells are surrounded by highly proliferative cells. In Fig. 3(e), the epithelium in the OCT images is too thin to make out much detail, however, there does appear to be some variation in the brightness of the epithelium. This may again be explained by the islands of terminally differentiated cells in the accompanying histology [Fig. 3(f)]. In Fig. 3(h), the model cultured from Cal27 cells had a very distinct appearance with the epithelium appearing in two layers. The most superficial of these layers was highly keratinized with an irregular surface topology that split on sectioning from a lower layer of more proliferative-looking/less-differentiated epithelial cells. This two-layer epithelium and the irregular surface topology is just visible in Fig. 3(g) with the two layers of the epithelium showing slightly different brightness intensities; again, the less-differentiated cells appearing darker (less backscattering) than the more-differentiated cells.

3.3 *Ability of OCT to Image Skin and Oral Mucosa In Vivo*

Figure 4 shows OCT images of a human fingertip [Fig. 4(a)] and the mucosal surface of the lower lip [Fig. 4(c)] obtained *in vivo* from a healthy volunteer, along with corresponding histology of human skin [Fig. 4(b)] and oral mucosa [Fig. 4(d)]. This was imaged using the SS-OCT system. In these images, features within the connective tissues can be distinguished including blood vessels and minor sweat and salivary glands. These features were

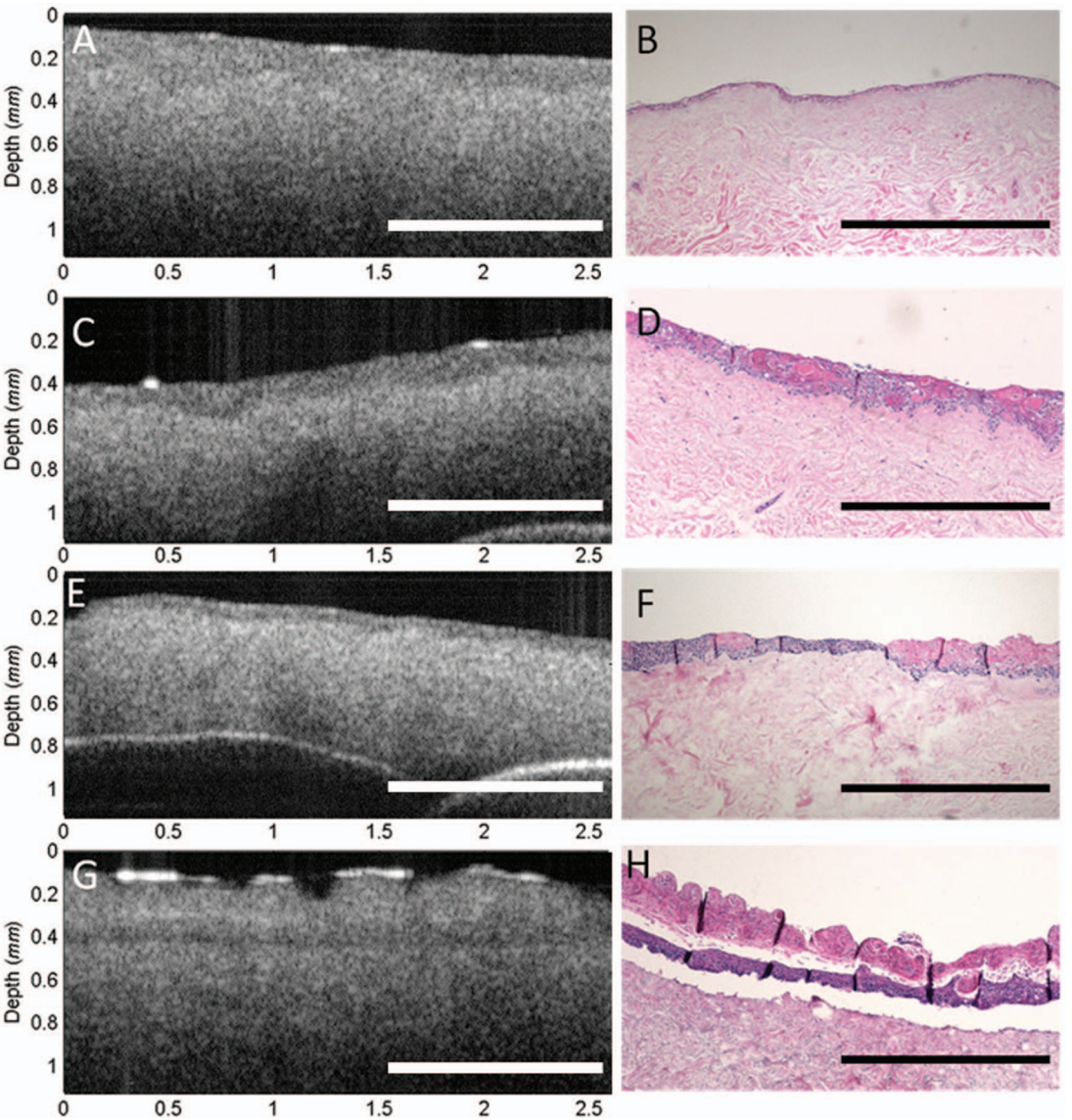

Fig. 3 (a) Representative SS-OCT image of TE oral mucosa and (b) accompanying histology. (c) Representative SS-OCT image of D20 model of invasive carcinoma and (d) accompanying histology. (e) Representative SS-OCT image of SCC9 model of severe dysplasia and (f) accompanying histology. (g) Representative SS-OCT image of Cal27 model of invasive carcinoma and (h) accompanying histology. All images were taken after the models had been at an air-liquid interface for 14 days. All histology stained with H&E. Scale bar = 1 mm.

more clearly imaged in the lip than in the skin. The OCT was able to obtain information over 500 μm deep in both the oral mucosa and skin, highlighting its potential to clinically diagnose both epithelial disorders, such as OSCC and SCC, but also submucosal conditions such as Sjögren's syndrome, which affects the salivary glands.

4 Discussion

Optical coherence tomography is a well-established technique for cross-sectional imaging of tissue, which is very successful in ophthalmology, but in areas such as dermatology, there are still challenges ahead.[20] We have previously shown that OCT can be successfully used to image TE skin[1,2,21] and we have also compared the imaging capabilities of OCT with other laboratory-based imaging techniques.[22] We have shown that OCT can be used to give experimental assurance about the development of TE skin, which is particularly valuable in experiments that may last for up to a month. However, we have not, until now, looked at whether OCT can be used to discriminate between normal and abnormal epithelia. In this study, we compared the ability of OCT to detect invasion of melanoma and OSCC in 3D models of TE skin and oral mucosa, respectively. Clearly, the ability of OCT to generate useful noninvasive information to detect epithelial abnormalities would be invaluable as many studies attest.[4,6,23–25] However, at present, the level of discrimination obtained with OCT in skin and oral mucosa remains close to being useful but falls short of something that could be routinely used for this purpose *in vitro* or *in vivo*.

Three-dimensional TE skin models constructed of cancer cell lines are useful experimental models in which to assess current OCT systems and also develop improvements to them. The

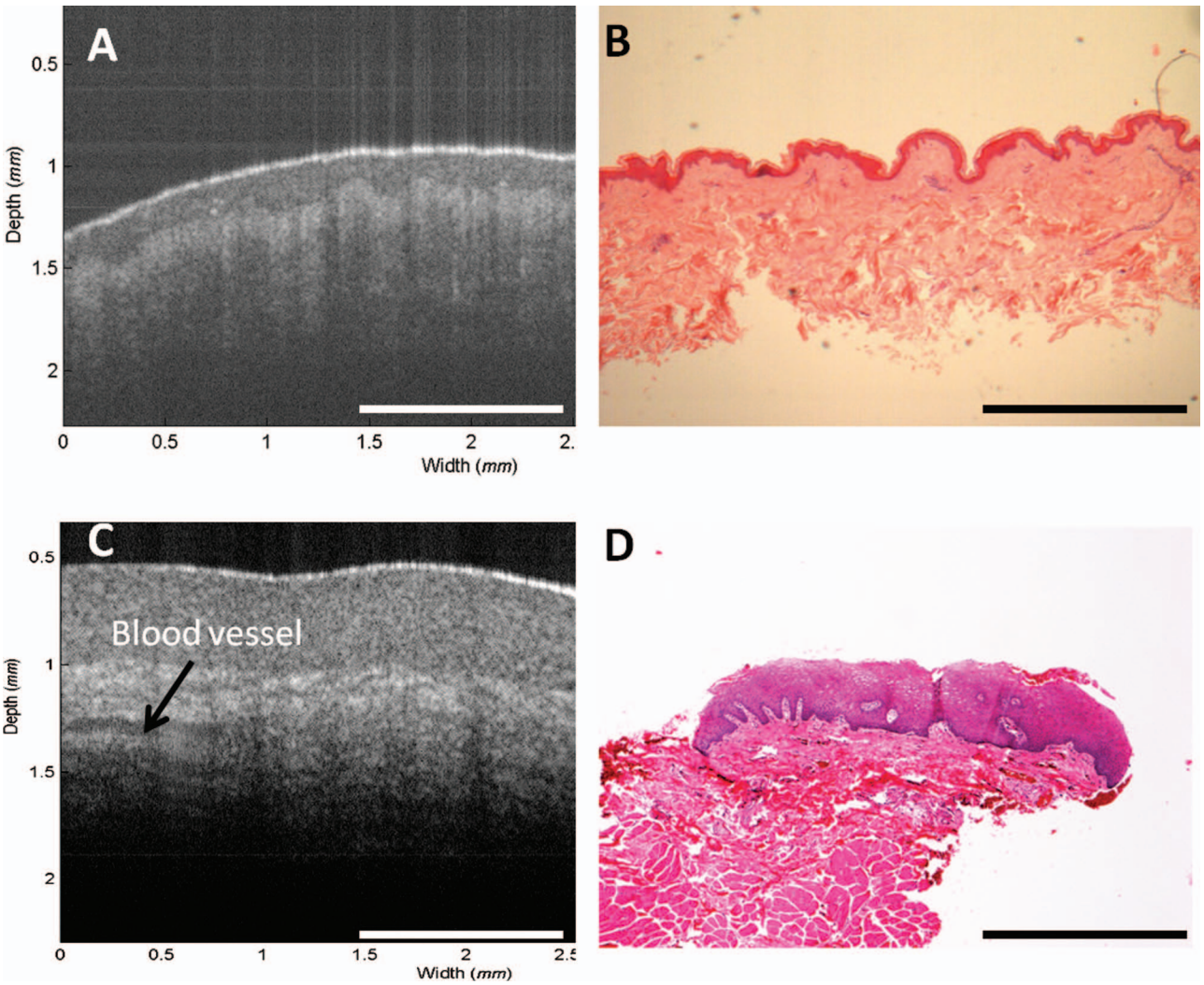

Fig. 4 (a) SS-OCT image of the skin of the finger tip *in vivo*. (b) Example histology of human skin. (c) SS-OCT image of the lower lip imaged *in vivo*. (d) Example histology of human oral mucosa. All histology stained with H&E. Scale bar = 1 mm.

three metastatic melanoma cell lines used in this study were HBL, A375-SM, and C8161 cell lines. Previous work in our group has shown that these cells have different invasive capabilities when cultured in three dimensions with human dermal fibroblasts and keratinocytes.[18,19] Of the three melanoma cell types, the HBL cells are minimally invasive, the A375-SM cells moderately invasive, and the C8161 cells highly invasive. For TE oral mucosa, again, three different oral cell lines were used, D20 a dysplastic cell line, and SCC9 and Cal27 both oral squamous cell carcinoma cell lines. When cultured in 3D, the D20 cells produce an epithelium that resembles a severe oral dysplasia (often a pre-cursor to oral cancer), while the SCC9 and Cal27 cell lines produce models resembling squamous cell carcinoma and become invasive when cultured longer.[26] The main finding of this study was that where there were gross disruptions to the epithelia of skin and oral models by the presence of cancer cells these were visible in the OCT images. These disruptions were comparable to disruptions seen with histological examination of tissue sections obtained from these samples. OCT did not, however, provide adequate resolution to discriminate between alterations in the epithelium caused by cancer cells compared to normal TE epithelium. The level of discrimination that we obtained was slightly better in the oral TE samples than in the skin TE samples, perhaps giving a clue to some of the problems that must be overcome.

Skin is not an ideal optical medium. It is optically complex, variable, and multilayered, which poses many problems to imaging.[24] It was evident that the images of skin *in vivo* on a fingertip were clearer than the images obtained from the *in vitro* TE model. It has been previously noticed that *ex vivo* and *in vitro* samples do not give as clear OCT images compared to *in vivo* images.[21] Hsiung et al. looked at the image quality degradation over time post-excision and found a reduction in signal intensity within a matter of hours. This was attributed to a loss of blood-flow, cell lysis, and subsequent changes in the tissue's microstructure.[27] It has been suggested that where keratin is packed tightly, such as in the fingertip stratum corneum, the OCT image would be expected to be less intense/less scattering, due to lack of changes in the index of refraction. However, in the TE constructs where the keratin is looser and mixed with cellular regions, air, or media, the keratinized regions might be expected to be more intense/more scattering. This appears

to occur in the OCT images in Figs. 1 and 2. For clinical applications, image degradation post excision is not a problem as real-time, noninvasive imaging is the ultimate aim. However, this may explain the difference in image quality obtained from TE models compared to *in vivo* tissue. Further clinical studies need to be undertaken to study, in more detail, the different appearances that arise from OCT imaging of different stages of OSCC and other potentially malignant mucosal conditions, as well as testing the specificities and sensitivities that can be achieved. OCT devices are still a relatively new technology and, for the most part, have been optimized for ocular applications. OCT development directed for oral or skin applications may further improve the images that can be obtained.

The ability of OCT to image differences in TE models of OSCC was also evaluated in this study. Tissue-engineered models such as these were able to give clear images of some features of the epithelium, such as the boundary of epithelium and connective tissue. Images taken *in vivo*, again appeared clearer and more features (many of which were not present in TE models) were visible, for example blood vessels.

Pathologically, the appearance of the epithelial connective tissue junction is important when diagnosing a number of different conditions, not just OSCC. Many mucosal diseases, including lichen planus, affect the junction between the epithelium and connective tissue and the diagnosis of these conditions may also benefit from OCT investigation. The ability to visualize not just the epithelium but also the adjacent connective tissue including blood vessels, ducts, and minor salivary glands may mean OCT has potential for diagnosis of nonmalignant oral diseases such as oral ulcerative conditions, Sjögren's syndrome, vascular anomolier, superficial cystic lesions, submucous fibrosis, orafacial granulomatosis, and lichen planus.

OCT is already being used to clinically examine oral[28] and laryngeal[29] lesions. Studies have shown good sensitivity and specificity when detecting carcinoma *in situ* and OSCC.[30,31] Images of dysplastic lesions showed epithelial thickening, loss of epithelial stratification, and epithelial down-growth as compared with healthy oral mucosa. Areas of OSCC were identified by the absence or disruption of the basement membrane, an epithelial layer that was highly variable in thickness, with areas of erosion and extensive epithelial down-growth and invasion into the sub-epithelial layers.[32] It was noted by Tsai et al. that when the neoplasm can be classified as mild or moderate dysplasia, there is a clear boundary between the epithelium and connective tissue, which disappears upon development of OSCC.[31] This was also the case when imaging nondysplastic lesions of the larynx, epithelial thickening with a defined basement membrane for benign lesions, and a loss of basement integrity with the development of laryngeal cancer.[29]

Given these findings, it is hoped that OCT may help to define surgical margins, reduce the need for investigative biopsies, and provide direct evaluation of the effectiveness of cancer treatments in the future.[28] OCT might also be used to image the whole oral cavity of a patient with a malignant lesion and find other areas of malignancy in the oral cavity that may not be observed by the naked eye. OCT could also be used by the clinician to monitor areas of dysplasia, which could help in the long term management of oral lesions and may avoid the necessity for regular repeat biopsy of these lesions.[33] Another major advantage over biopsy is the ability to produce real-time, point of care images of the tissues that can be discussed with the patient and enable efficient treatment planning and decision making without the need for a repeat visit as is needed following a biopsy.

In conclusion, OCT has the potential be a valuable tool in detecting epithelial abnormalities and, here, we demonstrate that it can detect major disruptions to the epithelial layer in both TE skin and oral mucosa. However, the system as used at present lacks the ability to detect more subtle perturbations or to detect cancer cells within the underlying connective tissue. However, this study does provide experimental models that can be used in future optimization studies to improve the resolution of the OCT systems currently available.

Acknowledgments

The authors would like to thank the BBSRC for supporting Dr. L.E. Smith (Grant No. BB/E002676/1), the EPSRC for supporting Dr. Z. Lu (Grant No. EP/F020422), and for providing a doctoral training award for V. Hearnden. The authors would also like to thank J. Holmes and S. Hattersley (Michelson Diagnostics Ltd., Orpington, Kent, United Kingdom) and Dr. M. Bonesi and Dr. N. Krstajić for useful discussions. The authors also thank the anonymous reviewers for helpful suggestions on image interpretation.

References

1. L. E. Smith, M. Bonesi, R. Smallwood, S. J. Matcher, and S. MacNeil, "Using swept-source optical coherence tomography to monitor the formation of neo-epidermis in tissue engineered skin," *J. Tissue Eng. Regener. Med.* **4**(8), 652–658 (2010).
2. L. E. Smith, Z. Lu, M. Bonesi, R. Smallwood, S. J. Matcher, and S. MacNeil, "Using swept source optical coherence tomography to monitor wound healing in tissue engineered skin," *Proc. SPIE* **7566**, 75660I (2010).
3. P. Wilder-Smith, M. J. Hammer-Wilson, J. Zhang, Q. Wang, K. Osann, Z. Chen, H. Wigdor, J. Schwartz, and J. Epstein, "*In vivo* imaging of oral mucositis in an animal model using optical coherence tomography and optical Doppler tomography," *Clin. Cancer Res.* **13**(8), 2449–2454 (2007).
4. P. Wilder-Smith, W. G. Jung, M. Brenner, K. Osann, H. Beydoun, D. Messadi, and Z. Chen, "*In vivo* optical coherence tomography for the diagnosis of oral malignancy," *Lasers Surg. Med.* **35**(4), 269–275 (2004).
5. M. T. Tsai, H. C. Lee, C. K. Lee, C. H. Yu, H. M. Chen, C. P. Chiang, C. C. Chang, Y. M. Wang, and C. C. Yang, "Effective indicators for diagnosis of oral cancer using optical coherence tomography," *Opt. Express* **16**(20), 15847–15862 (2008).
6. T. Gambichler, A. Orlikov, R. Vasa, G. Moussa, K. Hoffmann, M. Stucker, P. Altmeyer, and F. G. Bechara, "*In vivo* optical coherence tomography of basal cell carcinoma," *J. Dermatol. Sci.* **45**(3), 167–173 (2007).
7. M. Mogensen, T. M. Joergensen, B. Meincke Nurnberg, H. Ahmad Morsy, J. B. Thomsen, L. Thrane, and G. B. E. Jemec, "Assessment of optical coherence tomography imaging in the diagnosis of non-melanoma skin cancer and benign lesions versus normal skin: observer-blinded evaluation by dermatologists and pathologists," *Dermatol. Surg.* **35**(6), 965–972 (2009).
8. S. A. Boppart, W. Tan, H. J. Ko, and C. Vinegoni, "Optical coherence tomography of cell dynamics in three-dimensional engineered tissues," *Proc. SPIE* **5861**, 58610Z (2005).
9. W. Tan, T. A. Desai, D. Leckband, and S. A. Boppart, "Optical coherence tomography of cell dynamics in three-dimensional engineered tissues," *Proc. SPIE* **5699**, 102–110 (2005).

10. W. Tan, A. L. Oldenburg, J. J. Norman, T. A. Desai, and S. A. Boppart, "Optical coherence tomography of cell dynamics in three-dimensional tissue models," *Opt. Express* **14**(16), 7159–7171 (2006).
11. A. T. Yeh, B. Kao, W. G. Jung, Z. Chen, J. S. Nelson, and B. J. Tromberg, "Imaging wound healing using optical coherence tomography and multiphoton microscopy in an *in vitro* skin-equivalent tissue model," *J. Biomed. Opt.* **9**(2), 248–253 (2004).
12. F. Spöler, M. Forst, Y. Marquardt, D. Hoeller, H. Kurz, H. Merk, and F. Abuzahra, "High-resolution optical coherence tomography as a non-destructive monitoring tool for the engineering of skin equivalents," *Skin Res. Technol.* **12**(4), 261–267 (2006).
13. S. MacNeil, J. Shepherd, and L. Smith, "Production of tissue-engineered skin and oral mucosa for clinical and experimental use," in *3D Cell Culture: Methods and Protocols*, Vol. 695 of Methods in Molecular Biology, J. W. Haycock, Ed., Humana Press, Clifton, NJ (2011), pp. 129–153.
14. V. Hearnden, S. MacNeil, M. Thornhill, C. Murdoch, A. Lewis, J. Madsen, A. Blanazs, S. Armes, and G. Battaglia, "Diffusion studies of nanometer polymersomes across tissue engineered human oral mucosa," *Pharm. Res.* **26**(7), 1718–1728 (2009).
15. F. McGregor, A. Muntoni, J. Fleming, J. Brown, D. H. Felix, D. G. MacDonald, E. K. Parkinson, and P. R. Harrison, "Molecular changes associated with oral dysplasia progression and acquisition of immortality," *Cancer Res.* **62**(16), 4757–4766 (2002).
16. F. McGregor, E. Wagner, D. Felix, D. Soutar, K. Parkinson, and P. R. Harrison, "Inappropriate retinoic acid receptor-Î^2 expression in oral dysplasias: correlation with acquisition of the immortal phenotype," *Cancer Res.* **57**(18), 3886–3889 (1997).
17. K. H. Chakrabarty, R. A. Dawson, P. Harris, C. Layton, M. Babu, L. Gould, J. Phillips, I. Leigh, C. Green, E. Freedlander, and S. MacNeil, "Development of autologous human dermal-epidermal composites based on sterilized human allodermis for clinical use," *Br. J. Dermatol.* **141**(5), 811–823 (1999).
18. P. Eves, E. Katerinaki, C. Simpson, C. Layton, R. Dawson, G. Evans, and S. MacNeil, "Melanoma invasion in reconstructed human skin is influenced by skin cells - investigation of the role of proteolytic enzymes," *Clin. Exp. Metastasis* **20**(8), 685–700 (2003).
19. P. Eves, C. Layton, S. Hedley, R. A. Dawson, M. Wagner, R. Morandini, G. Ghanem, and S. MacNeil, "Characterization of an *in vitro* model of human melanoma invasion based on reconstructed human skin," *Br. J. Dermatol.* **142**, 210–222 (2000).
20. N. Krstajić, L. E. Smith, S. J. Matcher, D. T. D. Childs, M. Bonesi, P. D. L. Greenwood, M. Hugues, K. Kennedy, M. Hopkinson, K. M. Groom, S. MacNeil, R. A. Hogg, and R. Smallwood, "Quantum dot superluminescent diodes for optical coherence tomography: skin imaging," *IEEE J. Sel. Top. Quantum Electron.* **16**(4), 748–754 (2010).
21. N. Krstajić, J. Jacobs, M. Bonesi, L. E. Smith, P. Deshpande, S. MacNeil, R. Smallwood, and S. J. Matcher, "*Ex vivo* and *in vivo* OCT image contrast," *Proc. SPIE* **7139**, 71390W (2008).
22. L. E. Smith, R. Smallwood, and S. MacNeil, "A comparison of imaging methodologies for 3D tissue engineering," *Microsc. Res. Tech.* **73**(12), 1123–1133 (2010).
23. L. E. Smith and S. MacNeil, "REVIEW - State of the art in non-invasive imaging of cutaneous melanoma," *Skin Res. Technol.* **17**(3), 257–269 (2011).
24. M. Mogensen, L. Thrane, T. M. Joergensen, P. E. Andersen, and G. B. E. Jemec, "Optical coherence tomography for imaging of skin and skin diseases," *Semin. Cutan. Med. Surg.* **28**(3), 196–202 (2009)
25. W. Jerjes, T. Upile, B. Conn, Z. Hamdoon, C. S. Betz, G. McKenzie, H. Radhi, M. Vourvachis, M. El Maaytah, A. Sandison, A. Jay, and C. Hopper, "*In vitro* examination of suspicious oral lesions using optical coherence tomography," *Br. J. Oral Maxillofac. Surg.* **48**(1), 18–25 (2010).
26. H. E. Colley, V. Hearnden, A. V. Jones, P. H. Weinreb, S. M. Violette, S. MacNeil, M. H. Thornhill, and C. Murdoch, "Development of tissue engineered models of oral dysplasia and early invasive oral squamous cell carcinoma," *Br. J. Cancer* (in press).
27. P. L. Hsiung, P. R. Nambiar, and J. G. Fujimoto, "Effect of tissue preservation on imaging using ultrahigh resolution optical coherence tomography," *J. Biomed. Opt.* **10**(6), 064033 (2005).
28. P. Wilder-Smith, K. Lee, S. Guo, J. Zhang, K. Osann, Z. Chen, and D. Messadi, "In vivo diagnosis of oral dysplasia and malignancy using optical coherence tomography: preliminary studies in 50 patients," *Lasers Surg. Med.* **41**(5), 353–357 (2009).
29. T. Just, E. Lankenau, F. Prall, G. Huttmann, H. W. Pau, and K. Sommer, "Optical coherence tomography allows for the reliable identification of laryngeal epithelial dysplasia and for precise biopsy: a clinicopathological study of 61 patients undergoing microlaryngoscopy," *Laryngoscope* **120**(10), 1964–1970 (2010).
30. P. Wilder-Smith, J. Holtzman, J. Epstein, and A. Le, "Optical diagnostics in the oral cavity: an overview," *Oral Dis.* **16**(8), 717–728 (2010).
31. M. T. Tsai, C. K. Lee, H. C. Lee, H. M. Chen, C. P. Chiang, Y. M. Wang, and C. C. Yang, "Differentiating oral lesions in different carcinogenesis stages with optical coherence tomography," *J. Biomed. Opt.* **14**(4), 044028 (2009).
32. M. DeCoro and P. Wilder-Smith, "Potential of optical coherence tomography for early diagnosis of oral malignancies," *Expert Review of Anticancer Therapy* **10**(3), 321–329 (2010).
33. D. M. Keller, "Optical approaches to oral cancer screening and diagnosis: an expert interview with Petra Wilder-Smith, DDS, PhD," in *Medscape Medical News* (2010).